Impacts of climate change on hydrology in the Yellow River source region, China

Junliang Jin, Guoqing Wang, Jianyun Zhang, Qinli Yang, Cuishan Liu, Yanli Liu, Zhenxin Bao and Ruimin He

ABSTRACT

Variations of precipitation, temperature, and runoff in the Yellow River source region were analyzed with the Mann–Kendall and Spearman rank correlation tests over the past 60 years. Based on the seven climate scenarios from CMIP5 climate models under RCP2.6, RCP4.5, and RCP8.5, responses of hydrological process to climate change were simulated using the Variable Infiltration Capacity (VIC) model. Variation analysis results indicated that recorded temperature presented significant increasing trend. Daily minimum temperature presented higher increasing trend than daily maximum temperature. Annual gross precipitation presented minor increasing and annual runoff presented minor decreasing. The VIC model performed well on simulating monthly discharge at Tangnaihai station, with *NSE* of 0.91 and 0.93 in calibration and validation periods, respectively. The projected annual mean temperature would rise (with 25th and 75th percentiles) 1.07–1.32 °C, 1.76–2.33 °C, 3.45–4.29 °C, annual precipitation is expected to increase 3.43%–11.77%, 8.05%–17.27%, 12.84%–27.89%, and runoff would moderately increase with high variability of 0.82%–14.26%, −3.41%–19.14%, 1.43%–38.26% relative to the baseline of 1961–1990 under each RCP in the 2080s, respectively. The inhomogeneity of runoff may increase in the future. Many more droughts and floods under climate change may threaten social development in this region in the future.

Key words | climate change, hydrological responses, scenario, VIC, Yellow River source region

Junliang Jin (corresponding author)
Guoqing Wang
Jianyun Zhang
Qinli Yang
Cuishan Liu
Yanli Liu
Zhenxin Bao
Ruimin He
The State Key Laboratory of Hydrology-Water Resources and Hydraulic Engineering,
Nanjing Hydraulic research institute,
Nanjing, Jiangsu Province 210029,
China
E-mail: *jljin@nhri.cn*

Junliang Jin
Guoqing Wang
Jianyun Zhang
Cuishan Liu
Yanli Liu
Zhenxin Bao
Ruimin He
Research Center for Climate Change,
Ministry of Water Resources,
Nanjing, Jiangsu Province 210029,
China

Qinli Yang
School of Resources and Environment,
University of Electronic Science and Technology of China,
No. 2006 Xiyuan Avenue, Chengdu 611731,
China
and
Big Data Research Center,
University of Electronic Science and Technology of China,
No. 2006, Xiyuan Avenue, Chengdu 611731,
China

INTRODUCTION

Climate change is now a major environmental and developmental issue, and one that will increase the challenge of sustainable water resources management (Wang *et al.* 2012). Precipitation, evaporation, runoff, and soil moisture will be changed under global change environments. The issue of global warming has become an increasingly popular matter among society in recent years. Both the causes and effects of global warming have been the topic of heated debate not only among scientists, but also among politicians, businesses, and general members of society. Based on the Intergovernmental Panel on Climate Change Fifth Assessment Report (IPCC AR5) (IPCC 2013), the globally averaged combined land and ocean surface temperature data as calculated by a linear trend show a warming of 0.85 °C [0.65 to 1.06] over the period of 1880 to 2012, and presents a quickened warming pace in the past 30 years.

doi: 10.2166/wcc.2018.085

The World Meteorological Organization (WMO), United Nations Educational, Scientific and Cultural Organization (UNESCO) and International Association of Hydrological Sciences (IAHS) have prompted a series of science projects, such as World Climate Research Programme (WRCP), International Geosphere-Biosphere Program (IGBP), and International Hydrological Programme (IHP) in order to study the impact of climate change on water resources.

The potential impacts of global climate change on hydrological regimes and the distribution of water resources have been discussed widely in recent years. For example, Wang *et al.* (2012) assessed water resources in China using PRECIS projections and the Variable Infiltration Capacity (VIC) model. Ju *et al.* (2011) evaluated the accuracies of precipitation and temperature of 22 general circulation models (GCMs) from IPCC AR4 in China. Furthermore, many hydrological scientists have conducted relevant studies on the impact of climate change on water resources (Andreadis & Lettenmaier 2006; Zhang & Wang 2007; Su *et al.* 2016). Zhang *et al.* (2016) discussed the impacts of climate change on Xin River basin streamflows in China by using the SWAT model under RCP scenarios. They indicated that the average precipitation in three models showed slight and steady increase trends under RCP2.6 and RCP4.5, but a significant increase under the RCP8.5 scenario. Many RCPs also revealed a significant increase in monthly stream flow dispersion coefficient in October, reflecting a tendency for drought and flood events in that month. Guoqing's study presented the impact of climate change on water resources of the Yellow River basin by using the scenarios derived from CMIP3 and VIC models. (Wang *et al.* 2017). The result showed that runoff tended to increase for most of the upper reaches and the lower reaches of the Yellow River while runoff in the middle Yellow River basin tended to decrease with a higher decrease under scenarios A2 and B2. Otherwise, Hasan *et al.* (2018) discussed the runoff sensitivity to climate change in the Nile River basin. The results indicated that calculated runoff elasticities show that a 10% decrease in precipitation leads to a decrease in runoff of between 19% in the tropical zone and 30% in the arid zones. On the other hand, a 10% precipitation increase leads to a runoff increase of 14% in the tropical zone and 22% in the arid zone.

The Yellow River is always called the mother river of China. The source region of the Yellow River is the most important water sources conservation area. It is considered to be the major part of the water tower of China. The dataset analysis result shows that runoff of the source region accounts for more than 40% of the total Yellow River basin (Niu & Zhang 2005). People in the river basins and downstream depend directly on these water resources as a basis for their livelihoods, including for food production, hydropower, industry, and domestic supply. Thus, the hydrological cycle change of the source region will directly affect the water supply in the downstream of the Yellow River basin.

A number of observational studies have shown that streamflow measured at Tangnaihai decreased over the past decades (Cao *et al.* 2006; Tang *et al.* 2008; Hu *et al.* 2011). Cao *et al.* (2006) found that annual discharge at Tangnaihai station exhibited a statistically non-significant decreasing trend between 1956 and 2000. Seasonally, except for increases detected for April, May, and June, all other months exhibited decreases in discharge. Hu *et al.* (2011) analyzed streamflow at Tangnaihai station for a prolonged period of time (1959–2008), and found that streamflow decrease was associated with decreasing wet season (from May to September) precipitation and rising temperatures. Considering that the source region catchment was largely undisturbed by human activity, Hu *et al.* (2011) concluded that decreasing streamflow was predominantly caused by climate change. Furthermore, Zhang & Wang (2014) developed a grid-based VIC model using 56 sub-catchments located in the Huang-Huai-Hai area for model calibration and verification. The model works well for monthly natural discharge simulation for all sub-catchments as well as for the Yellow, Huai, and Hai river basins. The Nash–Sutcliffe efficiency coefficient of all sub-catchments ranges from 0.76 to 0.89 with relative errors varying from 4.1% to 3.7%. Variation of water resources in the Huang-Huai-Hai areas and the impact of climate change adaptive strategies have been reported by Wang & Zhang (2015), and they also indicated temperature in the Yellow River basin increased faster than the global average. Lu *et al.* (2013) assessed the impacts of future climate change on hydrology in the Huang-Huai-Hai region in China by using the PRECIS and VIC models and indicated extreme events such as droughts and severe floods could become more frequent in certain areas of this region. The impacts of climate change and land cover/use

transition on the hydrology in the upper Yellow River basin was discussed using the VIC model (Cuo *et al.* 2013). The upper Yellow River basin hydrological regimes have undergone changes over the past decades as reflected by a decrease in wet and warm season streamflow, and annual streamflow. VIC simulations suggest that these changes in observed streamflow were due to the combined effects of changes in precipitation and were caused primarily by climate change above the Tangnaihai hydrometric station. Uncertainty in projections of geographical and seasonal changes in climate is typically accounted for by using an ensemble of climate models. Under the CMIP, climate modeling groups have applied a number of climate models to produce an ensemble of estimates of change in climate for each RCP. A few studies have examined the impacts by using the CMIP5 (Coupled Model Intercomparison Project) phase 5 exercise (CMIP5: Taylor *et al.* 2012) of climate change and assessed the impacts on hydrology and hydrologic frequency in the Yellow River source region (YRSR).

The objectives of this study are: (1) to analyze historical hydro-meteorological data under climate change over the YRSR; (2) to investigate the impacts of climate change by applying a VIC model using projections of climate models in the future; (3) to explore the likely impacts of climate change on water resources.

Forcing the meteorological data into the hydrological model and analyzing the results of the model is the main method to assess the impact of climate change on district water resources. First, we analyzed the trend and characteristics of hydro-metro data over the past 60 years in the YRSR. The latest GCMs scenarios were used to force the hydrological model in order to predict the hydrological process in the future.

DATA AND METHODS

Study area

Located in the northeast of the Tibetan plateau, the YRSR is the hill catchment area of the Tangnaihai cross section. The watershed area of the YRSR is about 122,000 km^2. The length of the main river is over 300 km and the average slope is about 1.2‰. High mountains, canyons, and basins, lakes and swamp, and complicated topography exist in this region. There is high terrain in the west and low terrain in the east. As the long statistic data show, the mean annual gross precipitation is 485.9 mm. Yearly volume of runoff in the YRSR is 205.2×10^8 m^3, which accounts for about 40% of total natural runoff of the Yellow River basin. The YRSR is located in the sub-frigid zone of the Tibetan plateau with high temperature in the southeast and lower temperature in the northwest. This region has the feature of inland plateau weather characteristics.

Daily observed precipitation from 21 meteorological stations and 23 hydrological stations, daily maximum and minimum temperature from 21 meteorological stations, and daily discharge from the Tangnaihai hydrological station for the period 1951–2013 were collected in our study. Hydro-meteorology for the period 1951–2013 is used for trend analysis, and the period 1961–1990 is used for hydrological model calibration and validation.

Methods and data

Trend analysis and detection method

Temporal variabilities of annual precipitation and discharge along with temperature (maximum, minimum, and mean) were studied using multiple trend analysis techniques at 95% confidence level (significance level of 0.05) based on observing data of YRSR for a period of 63 years (1951–2013). The Mann–Kendall trend detection and Spearman rank correlation tests are both well developed methods for detecting hydro-meteorological features, so these two methods were used in our study. We aggregated the daily precipitation, maximum temperature, minimum temperature, average temperature, and discharge to annual average first. Then we detected the hydro-meteorological variabilities using methods similar to Sharma *et al.* (2016).

Description of variable infiltration capacity (VIC) model

The VIC model (Liang *et al.* 1994) was used to evaluate the hydrological process change over the YRSR in this study.

VIC is a macro-scale hydrologic model that solves full water and energy balances, and was originally developed by Xu Liang at the University of Washington. Its various forms have been applied to many watersheds including the Columbia River, Ohio River, Arkansas-Red Rivers, and Upper Mississippi Rivers, as well as being applied globally (Abdulla *et al.* 1996; Cherkauer & Lettenmaier 1999; Hamlet & Lettenmaier 1999; Liang & Xie 2003; Gergel *et al.* 2017; Li *et al.* 2017; Mote *et al.* 2018). The model was designed both for inclusion in GCMs as a land atmosphere transfer scheme, and for use as a stand-alone macro-scale hydrology model. Bao *et al.* (2012a, 2012b, 2012c) discussed the attribution for decreasing streamflow of the Haihe River basin and the impact of climate change and human activity on the Miyun Reservoir basin in China using the VIC model. Wu *et al.* (2007) and Wen *et al.* (2013) constructed past decades' daily soil moisture over China and Canada's prairies using the VIC model and achieved satisfactory results. Using the VIC model, Niu & Chen (2010) and Niu *et al.* (2013, 2014, 2015) simulated the terrestrial hydrological features of the Pearl River basin in South China for the period of 1952–2000, and also used the VIC model to investigate the impacts of increased CO_2 on the hydrologic response over the Xijiang (West River) basin, South China.

The VIC model divides a study catchment into grid cells, and then divides the soil column in each grid into three layers. The upper two layers, which are usually treated as one layer, are designed to represent the dynamic response of soil to rainfall events, while the lower soil layer is used to characterize seasonal soil moisture behavior. Three types of evaporation are considered: evaporation from wet canopy, evapotranspiration from dry canopy, and evaporation from bare soil. Stoma resistance is used to reflect the effects of radiation, soil moisture, vapor pressure deficiency, air temperature, etc. when calculating transpiration from the canopy.

The total runoff estimates consist of surface flow and base flow. Surface flow, including infiltration excess flow and saturation excess flow, is generated in the top two layers only. In order to consider the heterogeneity of soil properties, the soil storage capacity distribution curve and infiltration capacity curve are employed. The double curves are individually described as a power function with a B exponent. Base flow occurs in the lowest layer only, and is described by the Arno method (Habets *et al.* 1999) using the one-dimensional Richards equation to describe the vertical soil moisture movement. VIC structure and parameters are thus not discussed in this paper. A detailed introduction can be found on the VIC model website (http://vic.readthedocs.io/en/master/).

In this study, the VIC model was established over the YRSR at a spatial resolution of $0.5° \times 0.5°$ and daily temporal resolution (Figure 1). The model domain consists of 74 computational grid cells. A $0.5° \times 0.5°$ river network based on 1 km DEM was developed over the entire YRSR for purposes of defining the model's river routing scheme using the method of Lohmann *et al.* (1998), which takes daily VIC surface and subsurface runoff as input to obtain model simulated streamflows at the outlets of study basins.

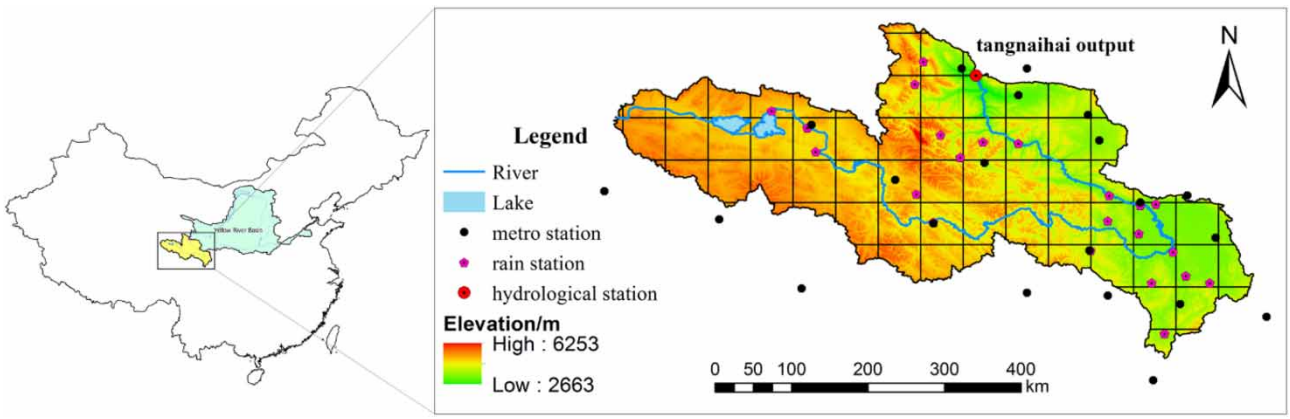

Figure 1 | Hydro-meteorological stations and grid cells in the Yellow River source region.

Climate change scenarios

A general circulation model (GCM) is the most important tool to predict future climate. The seven latest GCMs in current research were used in this study, namely, Beijing Climate Center Climate System Model version 1 (BCC-CSM1-1), Beijing Normal University Earth System Model (BNU-ESM), Centre National de Recherches Météorologiques Climate Model version 5 (CNRM-CM5), Goddard Institute for Space Studies Model E version 2 with Russell ocean model (GISS-E2-R), Model for Interdisciplinary Research on Climate- Earth System (MIROC-ESM), Max-Planck Institute Earth System Model-Low Resolution (MPI-ESM-LR), and Meteorological Research Institute Coupled GCM version 3 (MRI-CGCM3). Based on a set of experiments within CMIP5 and observed data, Xu & Xu (2012) assessed the performances of 18 global climate models on climate simulation over the 20th century in China and found that GCM models can capture the dominant features of the geographic distributions of temperature and precipitation during the years of 1961–2005. Among the 18 GCMs, CNRM and MIROC-ESM performed well on temperature simulation with the spatial correlation coefficient beyond 0.80 and temporal correlation coefficient reaching 95% confidence level. For the regional mean precipitation, CNRM achieved spatial correlation coefficient near 0.7 and spatial correlation efficiency beyond 0.8. Considering that the seven GCMs performed well in reproduction of temperature and precipitation in past decades over China, we selected them and the associated RCP scenarios in our research. These seven GCMs have metrological data over the whole study area under scenarios RCP2.6, RCP4.5, and RCP8.5 in the period of 1901–2100.

The three RCPs represent different trajectories of anthropogenic radiative forcing on the atmosphere. RCP2.6, RCP4.5, and RCP8.5, respectively, represent forcing data of 2.6, 4.5, and 8.5 W/m^2 by the year 2100. RCP2.6 has a peak forcing of 3 W/m^2 before declining to 2.6 W/m^2. RCP8.5 has the highest emission scenario used by IPCC AR5. RCP4.5 and RCP8.5 are the scenarios that stabilize radiative forcing at 4.5 W/m^2 and 8.5 W/m^2, respectively, in the year 2100 without ever exceeding that value. The RCPs differ not only in their radiative forcing but also in the assumed pathways for changes in aerosols.

Table 1 shows information on the seven GCMs used in this study. Scenarios have been constructed from the seven CMIP5 climate models which have been run for all three RCPs.

Table 1 | List of global circulation models

Number	Modeling group and model name	Originating group	Country
1	Beijing Climate Center Climate System Model version 1 (BCC-CSM1 – 1)	BCC, China Meteorological Administration	China
2	Beijing Normal University Earth System Model (BNU-ESM)	The College of Global Change and Earth System Science, BNU	
3	Centre National de Recherches Météorologiques Climate Model version 5 (CNRM-CM5)	CNRM/Centre Europeen de Recherche et Formation Avancees en Calcul Scientifique	France
4	Goddard Institute for Space Studies Model E version 2 with Russell ocean model (GISS-E2-R)	Goddard Institute for Space Studies, National Aeronautics and Space Administration	USA
5	Model for Interdisciplinary Research on Climate-Earth System (MIROC-ESM)	Atmosphere and Ocean Research Institute (AORI), National Institute for Environmental Studies, Japan Agency for Marine-Earth Science and Technology, Kanagawa	Japan
6	Max-Planck Institute Earth System Model-Low Resolution (MPI-ESM-LR)	Max-Planck Institute for Meteorology	Germany
7	Meteorological Research Institute Coupled General Circulation Model version 3 (MRI-CGCM3)	Meteorological Research Institute	Japan

The combination of bilinear-interpolation and delta method is applied in this study in order to calculate the gridded scenarios data with spatial resolution of $0.5^\circ \times 0.5^\circ$ from the coarse raw data (Liu *et al.* 2011). Meanwhile, the linear scaling approach aims to match the monthly mean of corrected values with that of observed values (Fang *et al.* 2015). Therefore, the linear scaling approach is used to correct the bias of precipitation and temperature of GCM scenarios' data in order to reduce the uncertainty in our study.

Metrological forcing data from scenario data including daily precipitation, daily maximum temperature, and daily minimum temperature with each RCP over the period of 1961 to 2100 are used to drive the VIC model. The model predicts the hydrological process in the 2030s, 2050s, and 2080s over the YRSR.

The methodology of impacts of climate change on hydrology includes three steps:

a) Define climate change scenarios from each of seven climate models forced with each RCP, representing change in 2021–2040 (2030s), 2041–2070 (2050s), and 2071–2099 (2080s) relative to 1961–1990.
b) Run the VIC model over the study area with the baseline climate and the future climates in daily time scale.
c) Aggregate the daily hydrological results to each period with the baseline and the future.

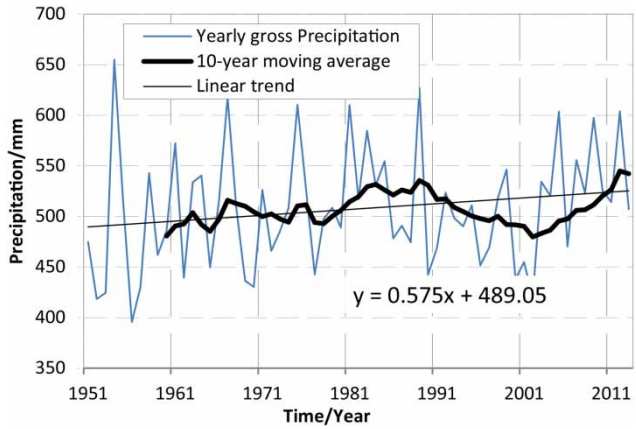

Figure 2 | Annual precipitation in the study area.

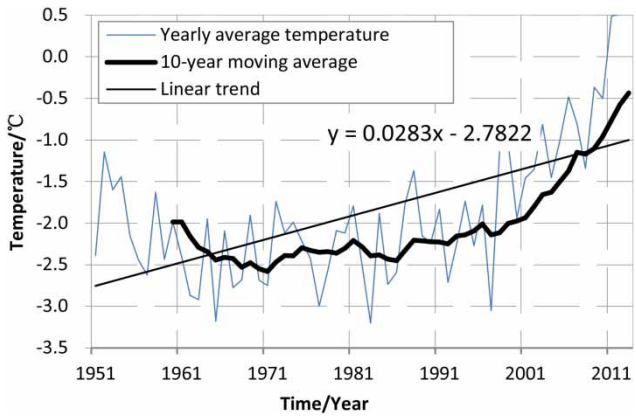

Figure 3 | Yearly average temperature in the study area.

RESULTS AND DISCUSSION

Historical variations of temperature, precipitation, and runoff

The long-term average annual precipitation and the mean temperature over the YRSR (Figures 2 and 3) during the period of 1951–2013 was about 507.4 mm and $-1.88\,^\circ$C, respectively.

Both the annual precipitation and the mean temperature had increasing trends of 0.475 mm/year and $0.028\,^\circ$C/year, respectively. The Mann–Kendall test for both series are 1.39 and 3.93, indicating the variation trends of the temperature series are not significant. The period of rapid temperature increase occurred after 1983.

Table 2 indicates the results of the meteorological data trend test over the YRSR. Annual precipitation, mean maximum temperature, and minimum temperature present increasing trends over the past 60 years. The annual runoff presents a decreasing trend. The daily mean minimum temperature shows a more obvious increasing trend than daily mean maximum temperature. The annual precipitation and annual runoff had slightly, but not significant, increasing and decreasing trends, respectively.

Discharge simulation

Soils, vegetation parameters, and hydrometeorology are required in the VIC model. We used the soils and vegetation parameters similar to Wang *et al.* (2012). Vegetation datasets are derived from Advanced Very High Resolution

Table 2 | Trend detection for hydro-meteorological data in the study area

Hydro-meteorological data	Average	Slope (/10a)	Spearman statistics	Mann–Kendall statistics	Trend
Annual precipitation	485.9 mm	4.76 mm	−1.39	1.39	Increase
Daily maximum temperature in annual average	2.55 °C	0.17 °C	−2.65*	2.54*	Increase
Daily minimum temperature in annual average	−12.21 °C	0.29 °C	−5.30*	4.85*	Increase
Daily mean temperature in annual average	−4.83 °C	0.23 °C	−4.18*	3.93*	Increase
Annual runoff	205.2×10^8 m^3	-6.85×10^8 m^3	1.78	−1.71	Decrease

Note: '*' indicates that the change trend of variable is significant.

Radiometer (AVHRR), which provides information on global land classification at 1 km resolution. Vegetation parameters, including architectural resistance, minimum stomata resistance, leaf-area index, albedo, roughness length, and zero-plane displacement, are derived mainly from the Land Data Assimilation System (LDAS). The classification of soil texture is based on global 5-min data provided by the National Oceanic and Atmospheric Administration (NOAA) hydrology office. The values for soil-related parameters, including porosity, saturated soil potential, and saturated hydraulic conductivity, are derived from the work of Cosby (1984) and Rawls & Yates (1976). As the VIC model is run through grid cells we aggregated the primitive soils and vegetation parameters to the spatial resolution of $0.5^\circ \times 0.5^\circ$ by GIS method in the beginning. The forcing data used for the VIC model include daily precipitation, air temperature, solar radiation, vapor pressure, and wind velocity. Due to the limited coverage of meteorological data, only daily precipitation and daily maximum and minimum air temperatures are used in our study, while other forcing terms are given default values. Daily precipitation and daily maximum and minimum air temperatures from 1951 to 2013 are interpolated by the inverse distance to a power gridding method to $0.5^\circ \times 0.5^\circ$ spatial resolution grids. The temperature dropping about 0.65 °C for every 100 m increase in altitude is considered when calculating the grid daily maximum and minimum air temperatures. Dataset series for daily discharge of Tangnaihai station and meteorological forcing data over the YRSB from 1961 to 1990 are divided into two periods: a calibration period from 1961 to 1980, and a validation period from 1981 to 1990. The start input forcing data of the model is ahead by one year in order to preheat the model's initial parameters, such as soil moisture.

There are many measures available to evaluate model performance. Zhang & Wang (2007) analyzed the advantages and shortcomings of four widely used model performance evaluation criteria: coefficient of correlation (R), Nash–Sutcliffe efficiency coefficient (NSE), root mean squared error ($RMSE$), and mean absolute percentage error ($MAPE$). The Nash–Sutcliffe efficiency criterion (Nash & Sutcliffe 1970) is a normalized statistic reflecting relative magnitude of the residual variance compared to the measured data variance. It is easy to compare the performance of hydrological models for different catchments with NSE. For the purpose of hydrological simulation and climate change study, it not only requires a good fit between observed and simulated runoff series, but also needs a good balance of total water mass. Therefore, the Nash–Sutcliffe efficiency criterion and the relative error (Er) of volumetric fit are employed as objective functions to calibrate the VIC model. A good simulation will result in values of NSE close to 1 and Er close to 0. The optimization procedure uses two objective functions:

$$\min Er = (\overline{Q_c} - \overline{Q_o})/\overline{Q_o} \times 100\% \quad (1)$$

$$\max NSE = 1 - \sum_i (Q_{i,c} - Q_{i,o})^2 / \sum_i (Q_{io} - \overline{Q_o})^2 \quad (2)$$

where $\overline{Q_c}$ and $\overline{Q_o}$ = time-averaged simulated and observed discharges, respectively; Er = relative error; $Q_{i,c}$ and $Q_{i,o}$ = simulated and observed discharge at time step (i), respectively; and NSE = Nash–Sutcliffe model efficiency coefficient. Manual intervention was used to define the initial values of parameters and analyze the rationality of the calibrated values of parameters.

The procedure of VIC calibration was similar to that of Wu *et al.* (2007). An auto optimization procedure based on

Rosenbrock (1960) was used under manual intervention during model calibration. We used basin observed daily discharges to calibrate the model because they reflect the integrated basin hydrological response. Most parameters of the VIC model were determined directly by geographical information (i.e., topography, vegetation, and soil) as mentioned above, whereas calibrations were required for the six VIC hydrologic parameters which are shown in Table 3. The thickness of the first soil moisture layer was kept constant (D1 = 0.1 m) and observed daily hydrographs from Tangnaihai station were used to calibrate the six parameters. We calibrated the six parameters of VIC through an auto optimization procedure based on Rosenbrock (1960). Six parameters were calibrated in turn until the *NSE* and *Er* reached the global optimization. After calibration, these six parameters remain unchanged and are used to simulate the discharge in the validation period 1981–1990. We aggregated daily discharge data to calculate monthly average discharge.

In order to test the performance of the VIC model with the transferred parameter values, the observed and simulated runoff at Tangnaihai station in calibration and validation are compared in Figures 4 and 5. The figures show that simulated and recorded runoff closely match for Tangnaihai station both in calibration and calibration periods. Table 3 shows the validated parameters and performance criteria at Tangnaihai station of the YRSR. Table 3 indicates *NSE* both in calibration and validation period exceeds 0.90, very near to 1, with the corresponding *Er* less than 3%. This indicates the calibration and validation results are satisfactory and the VIC model can simulate the hydrological process at the YRSR well. It can be used to assess the impact of climate change on hydrology in the YRSR.

Table 3 | The performance and validated parameters of VIC model at Tangnaihai station of YRSR

Types	Parameter descriptions	Value
Parameter	Variable infiltration curve (B)	0.38
	Maximum velocity of baseflow (Dm)	30
	Fraction of Dsmax where non-linear baseflow begins (Ds)	0.98
	Fraction of maximum soil moisture where non-linear baseflow occurs(Ws)	0.41
	Thickness of first soil moisture layer(D1)	0.10
	Thickness of second soil moisture layer(D2)	0.60
	Thickness of third soil moisture layer(D3)	0.59
Calibration (1961–1980)	*NSE*	0.91
	Er(%)	−2.42
Validation (1981–1990)	*NSE*	0.93
	Er(%)	0.92

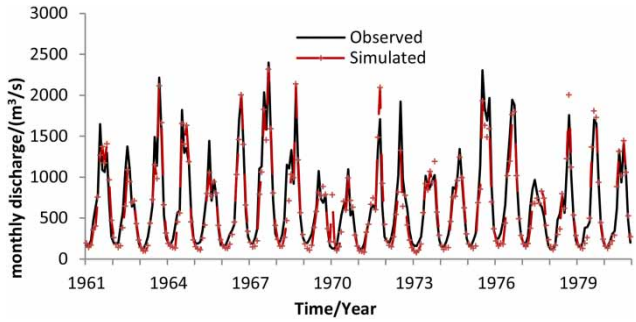

Figure 4 | The simulated and recorded monthly discharge during 1961–1980 of Tangnaihai station in calibration.

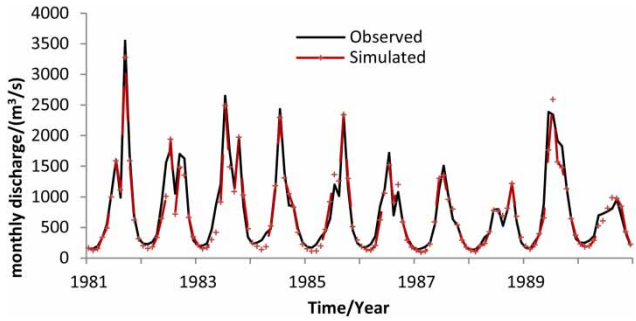

Figure 5 | The simulated and recorded monthly discharge during 1981–1990 of Tangnaihai station in validation.

Projected changes in future temperature and precipitation

Figures 6 and 7 show the changes in mean temperature and precipitation of the YRSR relative to 1961–1990 under the three RCPs, across the seven GCMs. The ensemble mean for each RCP is shown in the figures concurrently. The ensemble mean assumes all seven models are equally plausible.

Figure 6 indicates that projected annual mean temperature under the three emission scenarios rises steadily until mid century at an annual average rate of approximately 0.036 °C annum^{-1}, with the highest rate being 0.055 °C annum^{-1} under emission scenario RCP8.5. Temperature

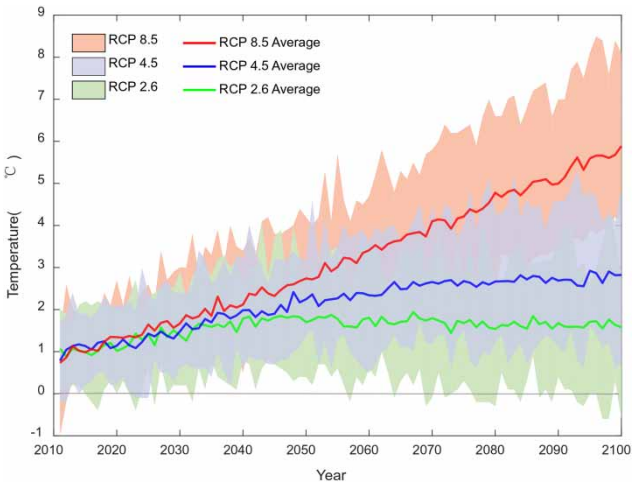

Figure 6 | Change in mean temperature of the YRSR, relative to 1961–1990, under the three RCPs.

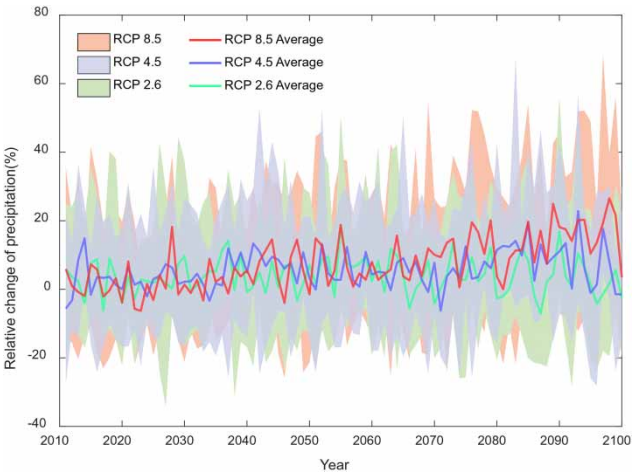

Figure 7 | Percentage change in mean precipitation of YRSR, relative to 1961–1990, under the three RCPs.

anomaly is about 1.65 °C to 2.99 °C until 2050 under the three emission scenarios, much higher than global rates cited by IPCC AR5 (IPCC 2013). Projected mean temperature rise will slow down and remain at a stable level in the second half of this century under emission scenarios RCP2.6 and RCP4.5. Unlike RCP2.6 and RCP4.5, projected mean temperature rise will increase steadily until the end of this century under emission scenario RCP8.5 with an annual average rate of approximately 0.060 °C annum^{-1}.

Figure 7 indicates that projected annual precipitation anomalies under the three emission scenarios are expected to rise slightly, with high variability (from −20% to 40%). On average, projected annual precipitation for the end of this century increases by 4.85%–18.70% compared with the baseline, 1961–1990. The coefficient of variation of annual precipitation will increase with time until the end of this century under the three emission scenarios.

Figures 8 and 9 show the spatial distribution of temperature (°C) and precipitation (%) anomaly, respectively, over the entire YRSR for the 2030s, 2050s, and 2080s with respect to the baseline, 1961–1990, under emission scenarios RCP2.6, RCP4.5, and RCP8.5. For the entire YRSR, annual temperature is projected to increase for all scenarios with the greatest warming in the north (exceeding 3.5 °C) and the least in the south (1.8–2.6 °C), with the larger warming occurring in the far future (2080s) under emission scenario RCP8.5. Annual precipitation is generally projected to increase by 0–10% in the near future (2030s), 5–15% in the mid century (2050s), 5–30% in the far future (2080s) with an increasing east–west gradient under different emission scenarios.

Figure 10 shows seasonal and mean annual changes in temperature and precipitation from the seven GCMs in the 2030s, 2050s, and 2080s compared with baseline under emission scenarios RCP2.6, RCP4.5, and RCP8.5, respectively. It exhibits large model variabilities for both temperature and precipitation, especially under the emission scenarios RCP4.5 and RCP8.5.

Figure 10 indicates that temperature is expected to rise rapidly based on all seven GCM scenarios. In general, projected temperature would increase from 1.07–1.32 °C, 1.76–2.33 °C, 3.45–4.29 °C under the emission scenarios RCP2.6, RCP4.5, and RCP8.5 in the far future (2080s), respectively (in annual means for the 25th and 75th percentiles range). The lower and middle emission scenarios (RCP2.6 and RCP4.5) have a moderate effect on future temperatures. The high emission scenario (RCP8.5) has a severe effect on the future temperature, particularly in the far distant period (2080s). The change in temperature magnitude in the far future is bigger than that in the near future. The change in temperature magnitude from the GCMs gives the different results, particularly under the emission scenario RCP4.5.

Annual precipitation is expected to rise slightly based on almost all scenarios, with high variability of 3.43%–11.77%, 8.05%–17.27%, 12.84%–27.89% under the emission scenarios RCP2.6, RCP4.5, and RCP8.5 in the far future of the

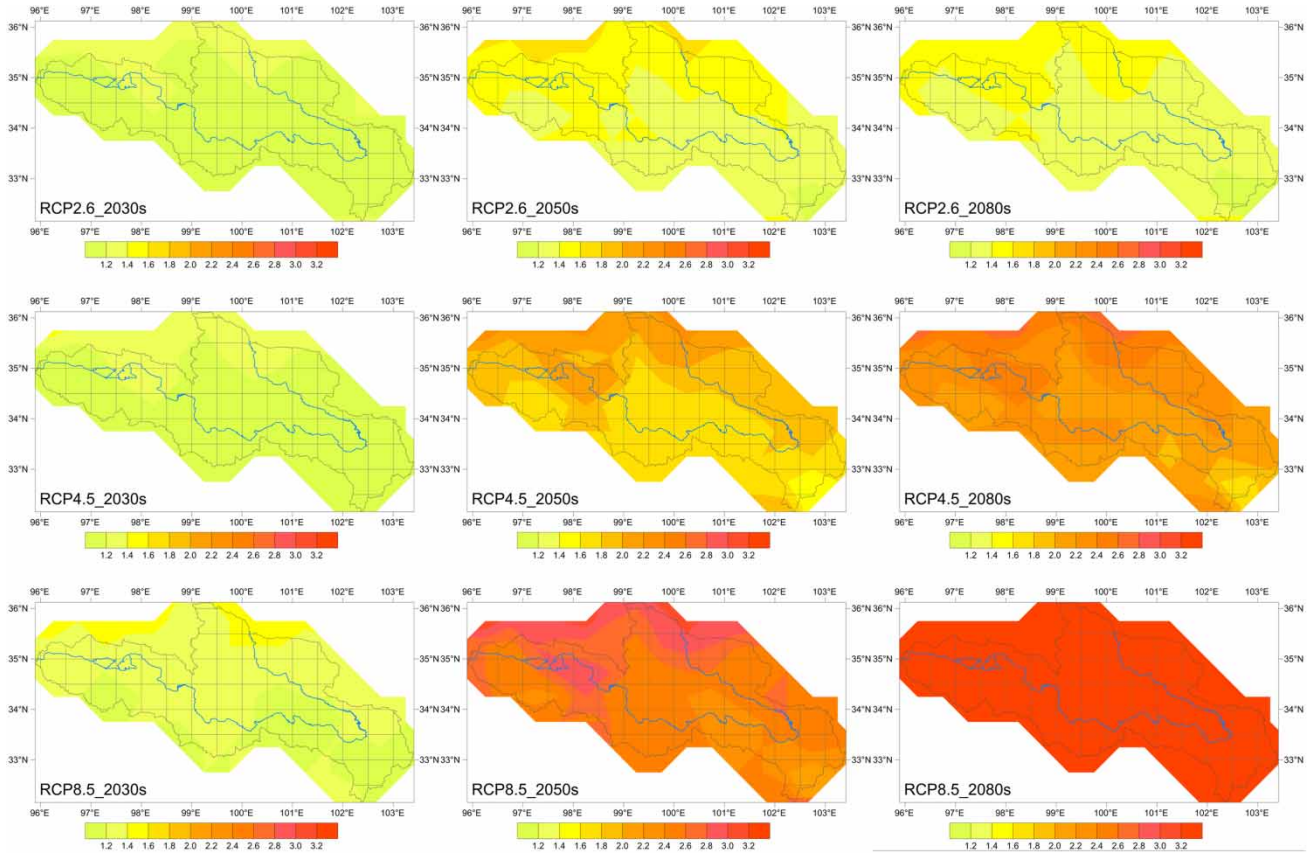

Figure 8 | Mean spatial temperature anomaly for the 2030s, 2050s, and 2080s related to the climate baseline period 1961–1990 for the emission scenarios RCP 2.6, RCP4.5, and RCP8.5 (°C).

2080s, respectively (in annual means for the 25th and 75th percentiles range). Along with time, annual precipitation under each scenario has a slightly increasing trend. The amplitude of annual precipitation will reach the peak, which is 21.10%, in the 2080s compared with the baseline under emission RCP8.5 for the 50th percentile.

In general, we can also find that winter has a much bigger increase in magnitude than the other seasons both in temperature and precipitation (Figures 8 and 9). Change amplitude of precipitation in summer is much smaller than that of the other seasons.

Projected changes in future runoff

Figure 11 shows the mean monthly runoff projections from the seven ensemble members in the 2080s under emission scenarios RCP2.6, RCP4.5, and RCP8.5. We summarize the ensemble projections by using a gray swath which spans the range of results from the seven ensemble members. We can find that the change of projected averaged annual runoff over the YRSR under the three emissions scenarios will slightly increase in the future. The trend under the three emission scenarios is almost the same. Despite the large spread among the runoff projections, the ensemble means generally show an increase in the future 2080s runoff relative to the baseline. For the specific period of the 2080s, the higher emission scenarios (RCP4.5 and RCP8.5) show more variation and uncertainty than the low emission scenario (RCP2.6). Runoff may be expected to rise based on the scenarios, with high variability of 0.82%–14.26%, −3.41%–19.14%, 1.43%–38.26% under the emission scenarios RCP2.6, RCP4.5, and RCP8.5 in the far future of the 2080s, respectively. The increased precipitation is the dominant cause of the total runoff increase.

The results are similar to past studies over this area by other researchers. Wang's study investigated the impact of

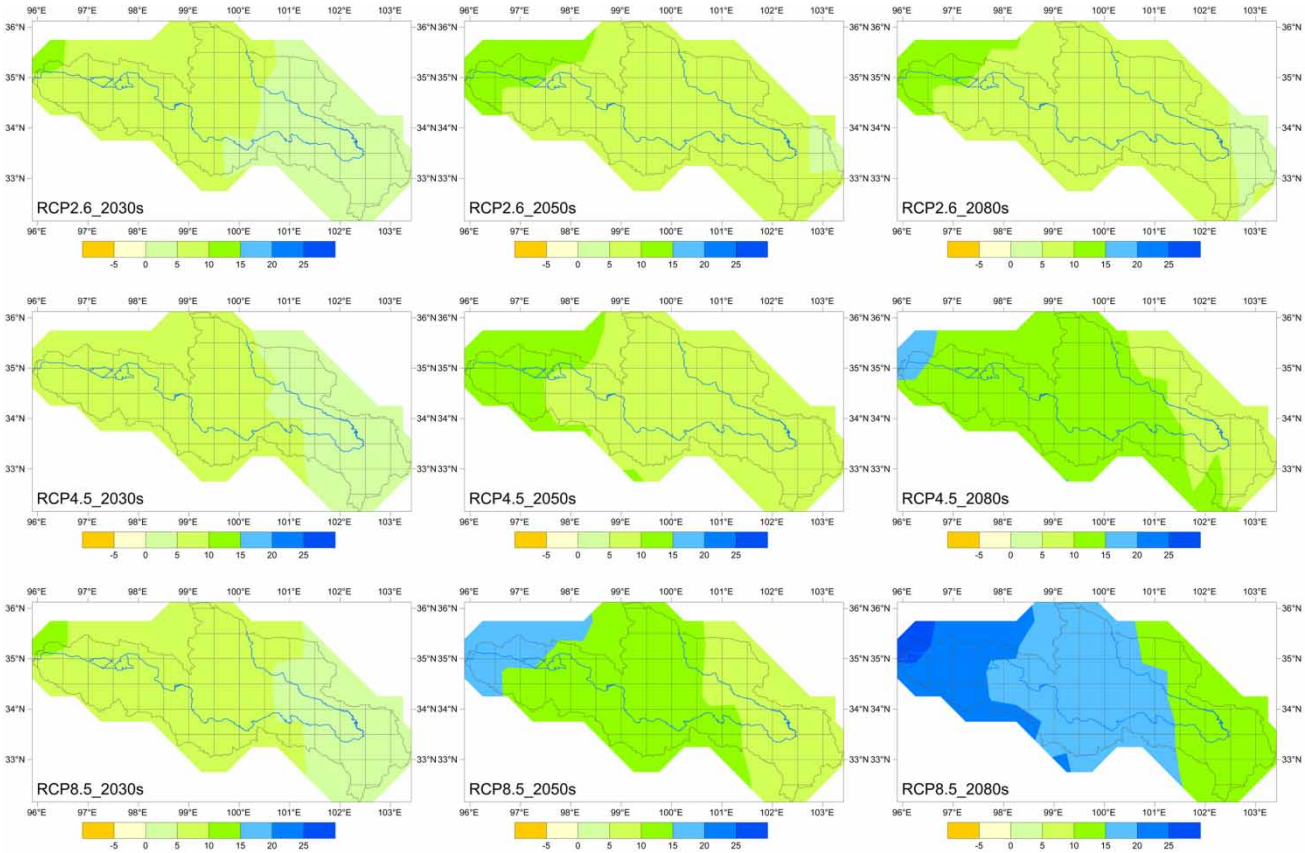

Figure 9 | Mean spatial precipitation anomaly for the 2030s, 2050s, and 2080s related to the climate baseline period 1961–1990 for the emission scenarios RCP 2.6, RCP4.5, and RCP8.5 (%).

climate change on water resources of the Yellow River basin by using the scenarios derived from the CMIP3 and VIC models. The result shows that runoff tends to increase for most of the upper reaches under scenarios A2 and B2 (Wang *et al.* 2017). Others have used different hydrological model and scenario data, such as the SWAT model, statistical downscaling model, and different kinds of GCMs from CMIP3 (e.g., Xu *et al.* 2009; Liu *et al.* 2011). Most of the conclusions indicate that the runoff over the YRSR will increase induced by future climate change in general.

Projected changes in future hydrologic frequency

The inner annual variation of runoff can be described by coefficient of variation.

$$C_v = \sigma\sqrt{R} \tag{3}$$

$$\sigma = \sqrt{\frac{1}{365}\sum_{i=1}^{365}(R_i - \bar{R})^2} \tag{4}$$

$$\bar{R} = \frac{1}{365}\sum_{i=1}^{365} R_i \tag{5}$$

where R_i is the daily discharge, $\bar{R}$ is the average annual discharge.

Figure 12 shows the coefficient of variation of daily discharge in the Tangnaihai station under the three emission scenarios. From Figure 11 we can know that the coefficient of variation increases with prolonged time. This means the inhomogeneity of daily discharge will increase slightly in the future, indicating that probability of extreme flood and drought events may increase in the future.

Although the impacts of climate change on future runoff and hydrologic frequency by using CMIP5 GCM scenarios and the VIC model present likely

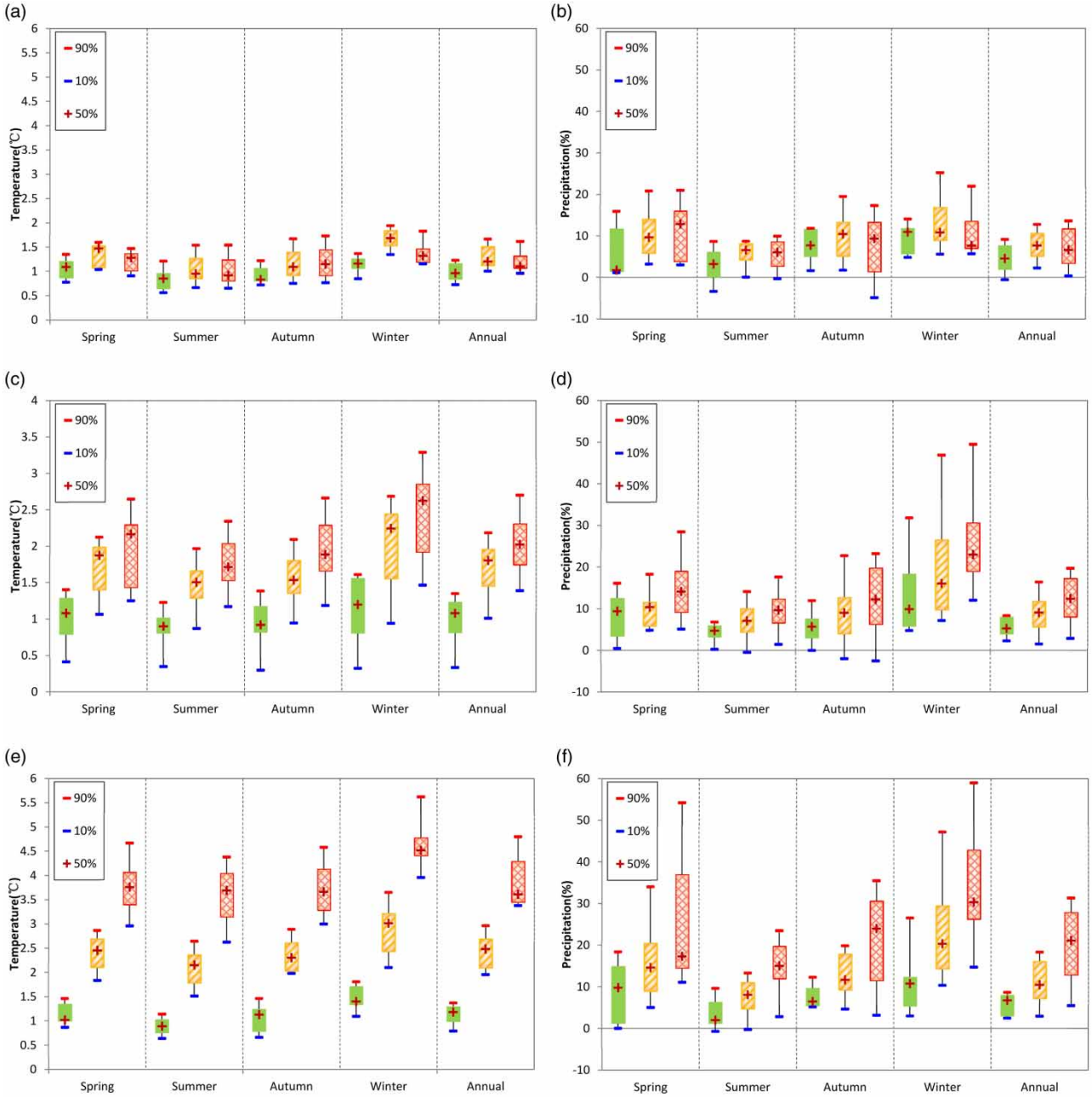

Figure 10 | Projected changes in temperature (°C) and precipitation (%) from seven CMIP5 GCMs for the 2020s, 2050s, and 2080s relative to baseline under emission scenarios RCP2.6, RCP4.5, and RCP8.5. The solid filled box indicates the 2030s, the oblique line filled box the 2050s, and the oblique grid filled box the 2080s. Box-and-whisker plots indicate the 10th and 90th percentiles (whiskers), 25th and 75th percentiles (box end), and median (solid +). (a) RCP2.6 temperature. (b) RCP2.6 precipitation. (c) RC4.5 temperature. (d) RCP4.5 precipitation. (e) RCP8.5 temperature. (f) RCP8.5 precipitation.

trends, these projections of future water resources still carry high uncertainty due to uncertainties in emission scenarios, in the outputs from GCMs, in downscaling approaches, and in the assessment model itself. The issue of uncertainty should therefore be addressed in further studies.

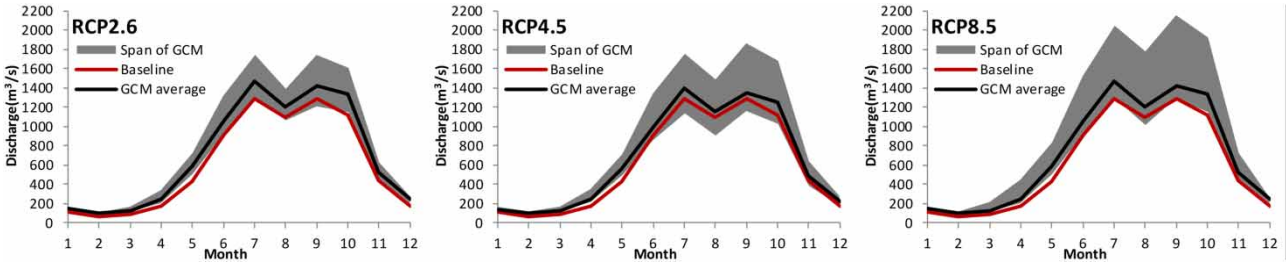

Figure 11 | Mean monthly runoff projections from seven GCMs ensemble scenarios for the 2080s period under RCP2.6, RCP4.5, and RCP8.5. The dotted line represents the ensemble means, the thick solid line represents the historic simulations for baseline, and the gray swath represents the span of results from the seven GCMs ensembles.

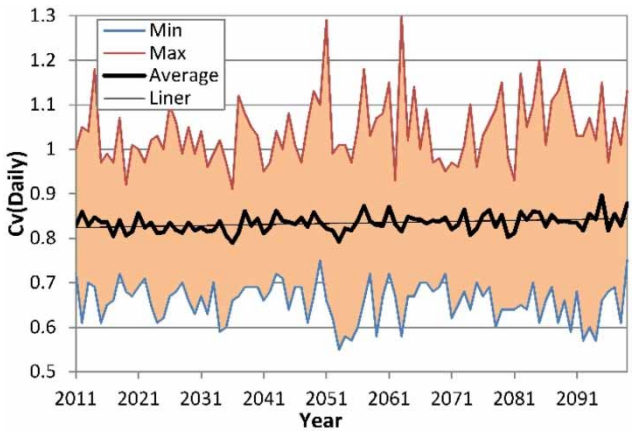

Figure 12 | The *Cv* of daily discharge in Tangnaihai station under three scenarios.

SUMMARY AND CONCLUSIONS

In this work, we detected the variabilities of historical precipitation, temperature, and runoff in the YRSR, then assessed the hydrological impacts' response to climate change in the YRSR by using the well-established VIC land surface hydrological model driven by composite projections of seven CMIP5 GCMs under scenarios RCP2.6, RCP4.5, and RCP8.5. The results are summarized as follows:

1. The temperature over the YRSR presents an obvious increasing trend during the past 60 years with a slope 0.23 °C/10 a which is bigger than 0.13 °C/10 a of increase over global land surface temperature warmed. Daily minimum temperature rising rate is bigger than the daily maximum temperature. The annual gross precipitation and the mean annual discharge present a slight increasing and decreasing trend, respectively.
2. The VIC model performed well on simulating monthly discharges at the Tangnaihai station in YRSR. *NSE* values in the calibration and validation period are 0.91 and 0.93, respectively, and the corresponding *Er* values are −2.42% and 0.92%.
3. The results using ensemble dataset from seven CMIP5 GCMs and three emission scenarios show that the temperature, precipitation, runoff, and the inhomogeneity of daily discharge will increase in the future. In annual means for the 25th and 75th percentiles range, projected temperature would increase 1.07–1.32 °C, 1.76–2.33 °C, 3.45–4.29 °C, annual precipitation is expected to rise slightly under most scenarios with high variability of 3.43%–11.77%, 8.05%–17.27%, 12.84%–27.89%, total runoff would either remain stable or moderately increase with high variability of 0.82%–14.26%, −3.41%–19.14%, 1.43%–38.26% relative to the baseline of 1961–1990 under the emission scenarios RCP2.6, RCP4.5, and RCP8.5 in the far future of the 2080s, respectively. The coefficient of variation increases and the inhomogeneity of daily discharge will increase slightly in the future.

The probability of flood and drought extreme events may increase in the future. The extreme hydrological events may threaten agriculture and animal husbandry in this region. Effective strategies for adaptation to climate change are essential for the sustainable development of water resources in the YRSR.

ACKNOWLEDGEMENTS

This study has been financially supported by the National Key R&D Program of China (grant no. 2017YFC0404401, 2016YFA0601501, 2017YFC0404403, 2017YFA0605002, 2017YFC1502706), the National Natural Science Foundation

of China (grant no. 51779144, 51679144, 51879164, 41401024, 41401026, 41330854, 41371063, 41501038, 41601025), the International Science & Technology Cooperation Program of China (grant no. 2010DFA24330), the Jiangsu Planned Projects for Postdoctoral Research Funds (grant no. 1101044C), the Fund on Basic Scientific Research Project of Nonprofit Central Research Institutions (grant no. Y514004, Y514010, Y516028) and State Key Laboratory of Hydrology-Water Resources and Hydraulic Engineering (grant no. 201801001). We are grateful to the three anonymous reviewers and editors for their valuable comments to improve the clarification of the paper.

REFERENCES

Abdulla, F. A., Lettenmaier, D. P., Wood, E. F. & Smith, J. A. 1996 Application of a macroscale hydrologic model to estimate the water balance of the Arkansas-Red river basin. *J. Geophys. Res.* **101**, 7449–7459.

Andreadis, K. M. & Lettenmaier, D. P. 2006 Trends in 20th century drought over the continental United States. *Geophys. Res. Lett.* **33** (10), 1–4.

Bao, Z., Fu, G., Wang, G., Jin, J., He, R., Yan, X. & Liu, C. 2012a Hydrological projection for the Miyun Reservoir basin with the impact of climate change and human activity. *Quat. Int.* **282**, 96–103.

Bao, Z., Zhang, J., Wang, G., Fu, G., He, R., Yan, X., Jin, J., Liu, Y. & Zhang, A. 2012b Attribution for decreasing streamflow of the Haihe River basin, northern China: climate variability or human activities? *J. Hydrol.* **460–461**, 117–129.

Bao, Z., Zhang, J., Liu, J., Fu, G., Wang, G., He, R., Yan, X., Jin, J. & Liu, H. 2012c Comparison of regionalization approaches based on regression and similarity for predictions in ungauged catchments under multiple hydro-climatic conditions. *J. Hydrol.* **466–467**, 37–46.

Cao, J., Qin, D., Kang, E. & Li, Y. 2006 River discharge changes in the Qinghai-Tibet Plateau. *Chinese Science Bulletin* **51** (5), 594–600.

Cherkauer, K. A. & Lettenmaier, D. P. 1999 Hydrologic effects of frozen soils in the Upper Mississippi River basin. *J. Geophys. Res.* **104**, 19599–19610.

Cosby, B. J. 1984 A statistical exploration of the relationships of soil moisture characteristics to the physical properties of soils. *Water Resour. Res.* **20**, 682–697.

Cuo, L., Zhang, Y., Gao, Y., Hao, Z. & Cairang, L. 2013 The impacts of climate change and land cover/use transition on the hydrology in the upper Yellow River Basin, China. *J. Hydrol.* **502**, 37–52.

Fang, G. H., Yang, J., Chen, Y. N. & Zammit, C. 2015 Comparing bias correction methods in downscaling meteorological variables for a hydrologic impact study in an arid area in China. *Hydrol. Earth Syst. Sci.* **11**, 2547–2559.

Gergel, D. R., Nijssen, B., Abatzoglou, J. T., Lettenmaier, D. P. & Stumbaugh, M. R. 2017 Effects of climate change on snowpack and fire potential in the western USA. *Clim. Change* **141**, 287–299.

Habets, F., Noilhan, J., Golaz, C., Goutorbe, J. P., Lacarrère, P., Leblois, E., Ledoux, E., Martin, E., Ottlé, C. & Vidal-Madjar, D. 1999 The ISBA surface scheme in a macroscale hydrological model applied to the Hapex-Mobilhy area-Part I: model and database. *J. Hydrol.* **217**, 75–89.

Hamlet, A. F. & Lettenmaier, D. P. 1999 Effects of climate change on hydrology and water resources in the Columbia River Basin. *Am. Water Res. Assoc.* **35**, 1597–1623.

Hasan, E., Tarhule, A., Kirstetter, P.-E., Clark III, R. & Hong, Y. 2018 Runoff sensitivity to climate change in the Nile River Basin. *J. Hydrol.* **561**, 312–321.

Hu, Y., Maskey, S., Uhlenbrook, S. & Zhao, H. 2011 Streamflow trends and climate linkages in the source region of the Yellow River, China. *Hydrol. Process.* **25** (22), 3399–3411.

IPCC 2013 *Climate Change 2013: The Physical Science Basis. Contribution of Working Group I to the Fifth Assessment Report of the Intergovernmental Panel on Climate Change*. Cambridge University Press, Cambridge, UK. New York, USA.

Ju, Q., Hao, Z.-c., Yu, Z.-b., Xu, H.-q., Jiang, W.-j. & Hao, J. 2011 Runoff prediction in the Yangtze River basin based on IPCC AR4 climate change scenarios. *Advances in Water Science* **22** (4), 462–469. (in Chinese with English abstract).

Li, D., Wrzesien, M. L., Durand, M., Adam, J. & Lettenmaier, D. P. 2017 How much runoff originates as snow in the western United States and how will that change in the future? *Geophys. Res. Lett.* **44**, 6163–6172.

Liang, X. & Xie, Z. 2003 Important factors in land–atmosphere interactions: surface runoff generations and interactions between surface and groundwater. *Global Planet Change* **38** (1–2), 101–114.

Liang, X., Lettenmaier, D. P. & Wood, E. F. 1994 A simple hydrologically based model of land surface water and energy fluxes for general circulation models. *J. Geophys. Res.* **99** (7), 14415–14428.

Liu, L., Liu, Z., Ren, X., Fischer, T. & Xu, Y. 2011 Hydrological impacts of climate change in the Yellow River Basin for the 21st century using hydrological model and statistical downscaling model. *Quat. Int.* **244**, 211–220.

Lohmann, D., Raschke, E. & Nijssen, B. 1998 Regional scale hydrology-I: formulation of the VIC-2 L model coupled to a routing model. *Hydrol. Sci. J.* **43**, 131–141.

Lu, G.-H., Heng, X., Wu, Z., Zhang, S.-L. & Li, Y. 2013 Assessing the impacts of future climate change on hydrology in Huang-Huai-Hai region in China using the PRECIS and VIC models. *J. Hydrol. Eng.* **18** (9), 1077–1087.

Mote, P. W., Li, S., Lettenmaier, D. P., Xiao, M. & Engel, R. 2018 Dramatic declines in snowpack in the western U.S. *NPJ Clim Atmos. Sci.* **2**, 1–6.

Nash, J. E. & Sutcliffe, J. V. 1970 River flow forecasting through conceptual models: part 1 - a discussion of principles. *J. Hydrol.* **10** (3), 282–290.

Niu, J. & Chen, J. 2010 Terrestrial hydrological features of the Pearl River basin in South China. *J Hydro-Environ Res.* **4**, 279–288.

Niu, Y.-g. & Zhang, X.-c. 2005 Preliminary analysis on variations of hydrologic and water resources regime and its genesis of the Yellow River Source Region. *Yellow River* **27** (3), 31–36. (In Chinese).

Niu, J., Sivakumar, B. & Chen, J. 2013 Impacts of increased CO_2 on the hydrologic response over the Xijiang (West River) basin, South China. *J. Hydrol.* **505**, 218–227.

Niu, J., Chen, J. & Sivakumar, B. 2014 Teleconnection analysis of runoff and soil moisture over the Pearl River basin in southern China. *Hydrol. Earth Syst. Sci.* **18**, 1475–1492.

Niu, J., Chen, J. & Sun, L. 2015 Exploration of drought evolution using numerical simulations over the Xijiang (West River) basin in South China. *J. Hydrol.* **526**, 68–77.

Rawls, W. & Yates, P. 1976 *Calibration of Selected Infiltration Equations for the Georgia Coastal Plain*. US Department of Agriculture, Agricultural Research Service, Washington, DC, USA, pp. 121–134.

Rosenbrock, H. H. 1960 An automatic method for finding the greatest or least value of a function. *Comput. J.* **3** (3), 175–184.

Sharma, C. S., Panda, S. N., Pradhan, R. P., Singh, A. & Kawamura, A. 2016 Precipitation and temperature changes in eastern India by multiple trend detection methods. *Atmos. Res.* **180**, 211–225.

Su, F., Zhang, L., Ou, T., Chen, D., Yaob, T., Tong, K. & Qi, Y. 2016 Hydrological response to future climate changes for the major upstream river basins in the Tibetan Plateau. *Global Planet Change* **136**, 82–95.

Tang, Q., Oki, T., Kanae, S. & Hu, H. 2008 Hydrological cycles change in the Yellow River Basin during the last half of the twentieth century. *J. Clim.* **21**, 1790–1806.

Taylor, K. E., Stouffer, R. J. & Meehl, G. A. 2012 An overview of CMIP5 and the experiment design. *Bull. Am. Meteorol. Soc.* **93**, 485–498.

Wang, G. Q. & Zhang, J. Y. 2015 Variation of water resources in the Huang-huai-hai areas and adaptive strategies to climate change. *Quat. Int.* **380–381**, 180–186.

Wang, G. Q., Zhang, J. Y., Jin, J. L., Pagano, T. C., Calow, R., Bao, Z. X., Liu, C. S., Liu, Y. L. & Yan, X. L. 2012 Assessing water resources in China using PRECIS projections and a VIC model. *Hydro. Earth Syst. Sci.* **16**, 231–240.

Wang, G., Zhang, J., Jin, J., Weinberg, J., Bao, Z., Liu, C., Liu, Y., Yan, X., Song, X. & Zhai, R. 2017 Impacts of climate change on water resources in the Yellow River basin and identification of global adaptation strategies. *Mitig. Adapt. Strat. Glob. Change* **22** (1), 67–83.

Wen, L., Lin, C. A., Wu, Z., Lu, G., Pomeroy, J. & Zhu, Y. 2013 Reconstructing sixty year (1950-2009) daily soil moisture over the Canadian Prairies using the Variable Infiltration Capacity model. *Can. Water Res. J.* **36** (1), 83–102.

Wu, Z., Lu, G., Wen, L., Charles, A. L., Zhang, J. & Yang, Y. 2007 Thirty-five year (1971–2005) simulation of daily soil moisture using the variable infiltration capacity model over China. *Atmos. Ocean.* **45** (1), 37–45.

Xu, Y. & Xu, C.-H. 2012 Preliminary assessment of simulations of climate changes over China by CMIP5 multi-models. *Atmos. Ocean. Sci. Lett.* **5**, 489–494.

Xu, Z. X., Ahao, F. F. & Li, J. Y. 2009 Response of streamflow to climate change in the headwater catchment of the Yellow River basin. *Quat. Int.* **208**, 62–75.

Zhang, J.-Y. & Wang, G. 2007 *The Impacts of Climate Change to Water Resources*. China Science Press, Beijing. (In Chinese)

Zhang, J. Y. & Wang, G. Q. 2014 *Variation of Stream Flow and Quantitative Identification for Attribution*. Science Press, Beijing. (In Chinese).

Zhang, Y., You, Q., Chen, C. & Ge, J. 2016 Impacts of climate change on streamflows under RCP scenarios: a case study in Xin River Basin, China. *Atmos. Res.* **178–179**, 521–534.

First received 2 April 2018; accepted in revised form 15 August 2018. Available online 3 September 2018